A stochastic 3D microstructure model for loam and sand based on Gaussian random fields: Investigating microstructure-property relationships

Matthias Weber

Institute of Stochastics, Ulm University, Ulm

Fall School Time Series, Random Fields and beyond | 26th September 2024

Introduction

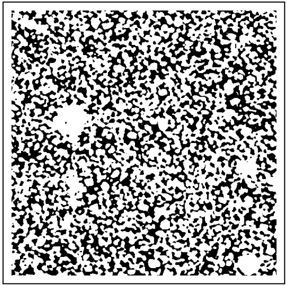

(a) 2D cross-section of (binarized) 3D CT of soil.

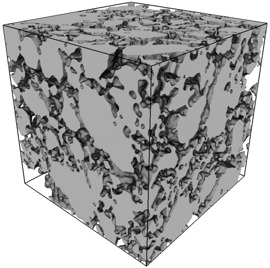

(b) 3D rendering of (binarized) 3D CT of soil.

Diffusion in soils

Diffusive processes play an important role in nutrient transport in soil. How are these processes linked to geometric descriptors of pore space?

Overview

Model

Model description
Model fitting
Model validation

Microstructure-property relationships

Statistical description of data
Functional relationships

Conclusion

Model description

Two independent *stationary* and *isotropic Gaussian* random fields $\{X_1(t), t \in \mathbb{R}^3\}$ and $\{X_2(t), t \in \mathbb{R}^3\}$

- with mean values μ_i and *covariance functions* $C_i : [0, \infty) \to \mathbb{R}$ with $i \in \{1, 2\}$
- normalized, i.e., $\mu_i = 0$ and $C_1(0) = C_2(0) = 1$

Matern covariance functions:

$$C_i(d) = \frac{2^{1-\nu_i}}{\Gamma(\nu_i)} \left(\sqrt{2\nu_i} \frac{d}{\rho_i} \right)^{\nu_i} K_{\nu_i} \left(\sqrt{2\nu_i} \frac{d}{\rho_i} \right),$$

with $\nu_i > 0$ and $p_i > 0$.

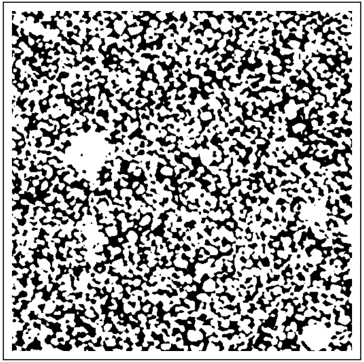

Model description

Random closed sets $\Xi_i = \{t \in \mathbb{R}^3 : X_i(t) \geq a_i\}$ (*level sets*) for some $a_i \in \mathbb{R}$

- with volume fractions $\varepsilon_i > 0$
- $\varepsilon_i = 1 - \Phi(a_i)$, where $\Phi : \mathbb{R} \to [0, 1]$ denotes the cumulative distribution function of the univariate standard normal distribution

Model the solid phase as $\Xi = \Xi_1 \cup \Xi_2$

- with volume fraction $\varepsilon = \varepsilon_1 + \varepsilon_2 - \varepsilon_1 \varepsilon_2$

The resulting model has six parameters: $\varepsilon_i, \rho_i, \nu_i$ for $i \in \{1, 2\}$

Model description

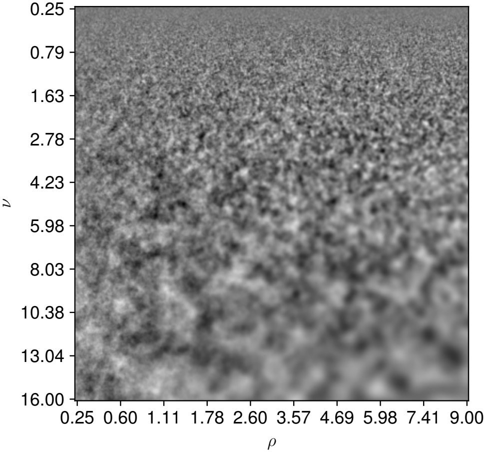

(a) Illustration of X for different values of ρ and ν.

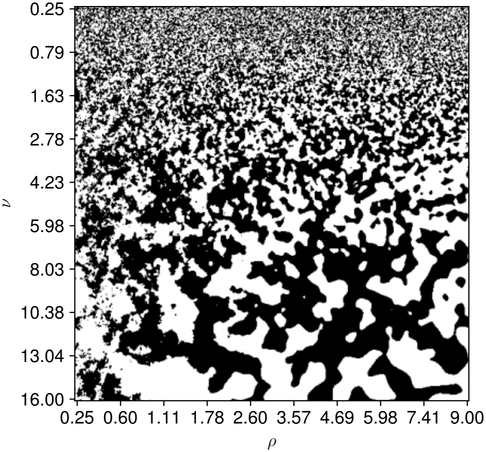

(b) Level set Ξ for $\varepsilon = 0.5$.

Model description

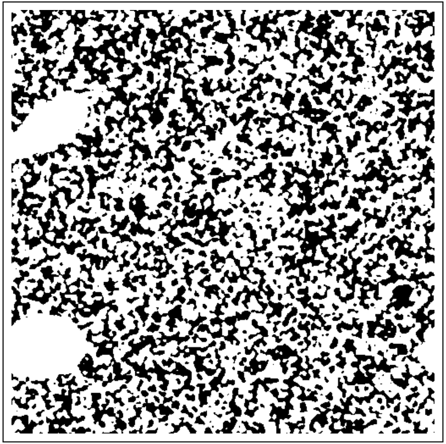

2D slice of a realization of the model.

Model fitting: Chord length distribution

For a random closed set $\Xi \subset \mathbb{R}^2$, the distribution of chord lengths in direction e_2 is usually defined as

$$L_{e_2}(r) = 1 - \frac{\mathbb{E}(X(((\Xi \cap g(\mathbb{R})) \ominus g([0,r])) \cap [0,1]^2))}{\mathbb{E}(X(\Xi \cap g([0,1])))},$$

for $r > 0$, where $g(A) = \{0\} \times A$ for $A \in \mathcal{B}(\mathbb{R})$ and $X(B)$ denotes the number of connected components of $B \in \mathcal{B}(\mathbb{R})$. Essentially, this is *"counting" chords* of at most length r.

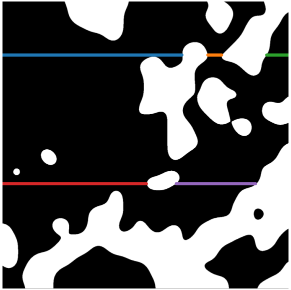

Using this definition, short chords are overrepresented in comparison to long chords.

Model fitting: Chord length distribution – length weighted

The overrepresentation of short chords can be overcome by considering the length-weighted chord length distribution. Essentially, this is

$$\tilde{L}_{e_2}(r) = \mathbb{P}(l_{e_2}(0) \leq r)\,,$$

where $l_{e_2}(x)$ is the length of the chord in direction e_2 through x.

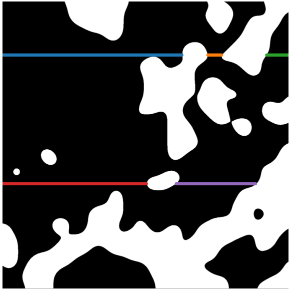

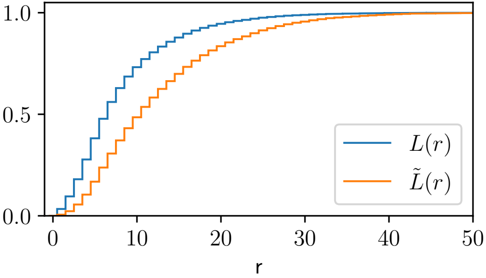

Model fitting

Consider the probability densities

$$l_{data,pore}, l_{data,solid}, l_{\xi,pore}, l_{\xi,solid} : [0, \infty) \to \mathbb{R}$$

corresponding to the (length-weighted) chord length distributions estimated for the pore and solid phase of measured *data* and a simulated model realization ξ, respectively. Then, define a cost function

$$H(\xi) = \|l_{data,pore} - l_{\xi,pore}\|_{L^2}^2 + \|l_{data,solid} - l_{\xi,solid}\|_{L^2}^2 .$$

For the given data, optimiziation inspired by simulated annealing yields the parameters $\varepsilon_1 = 0.04, \varepsilon_2 = 0.57, \rho_1 = 70.07, \nu_1 = 44.63, \rho_2 = 2.86, \nu_2 = 82.14.$

Model validation

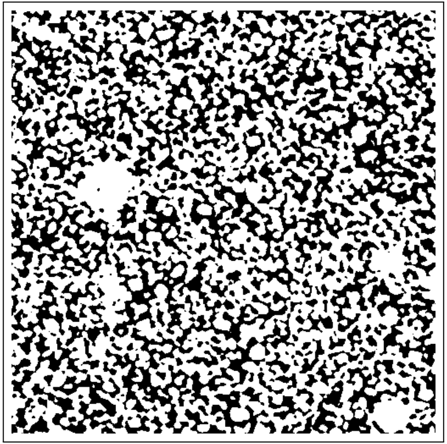

(a) 2D cross-section of CT data of sand.

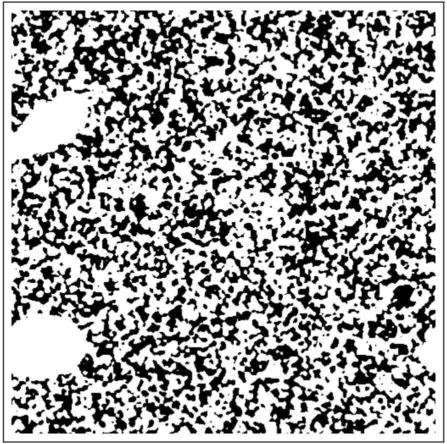

(b) 2D cross-section of simulated structure.

Model validation

Validation using geometric descriptors:

descriptor	measured	simulated
ε	0.586	0.583
S	0.215	0.212
$\mu(C)$ (pore) *	7.845	7.775
$\mu(C)$ (solid) *	10.955	10.883
$\mu(\tau)$	1.090	1.098
$\sigma(\tau)$	0.00674	0.00957
$\beta = (r_{min}/r_{max})^2$	0.514	0.452

* used for fitting

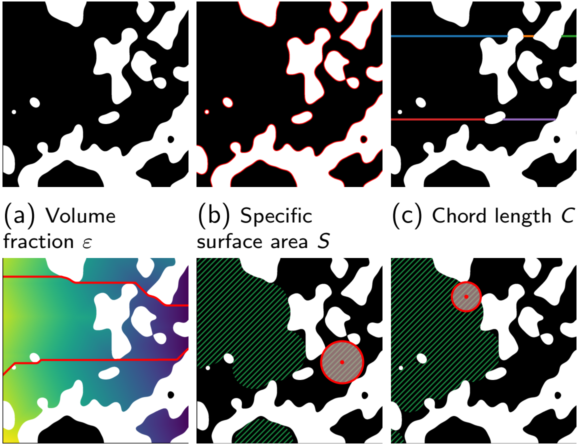

(a) Volume fraction ε (b) Specific surface area S (c) Chord length C

(d) Tortuosity τ (e) r_{max} (f) r_{min}

Illustrations of geometric descriptors.

Microstructure-property relationships

Investigate how diffusion is linked to microstructure descriptors:

- Consider data of *loam* and *sand*
- Fit parametric prediction formulas

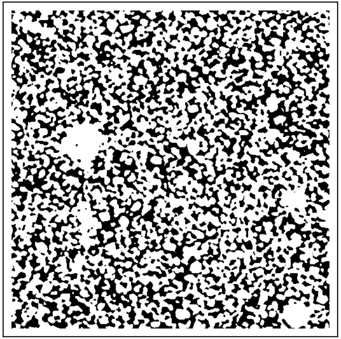

(a) 2D cross-section of CT data of sand.

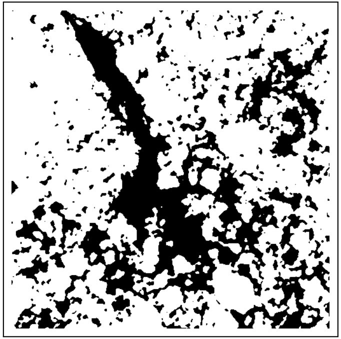

(b) 2D cross-section of CT data of loam.

Microstructure-property relationships

The datasets of loam and sand were split into a total of 2676 non-overlapping cutouts.

On each cutout, *geometric descriptors* were computed. The effective diffusion tensor $\mathbb{D} \in \mathbb{R}^{3\times 3}$ was calculated by numerically solving the Laplace equation and the *M-factor* was obtained by

$$M = \frac{1}{3D_m}(\mathbb{D}_{1,1} + \mathbb{D}_{2,2} + \mathbb{D}_{3,3}) \in [0,1]\,,$$

where $D_m > 0$ is the molecular diffusivity.

Statistical description of data

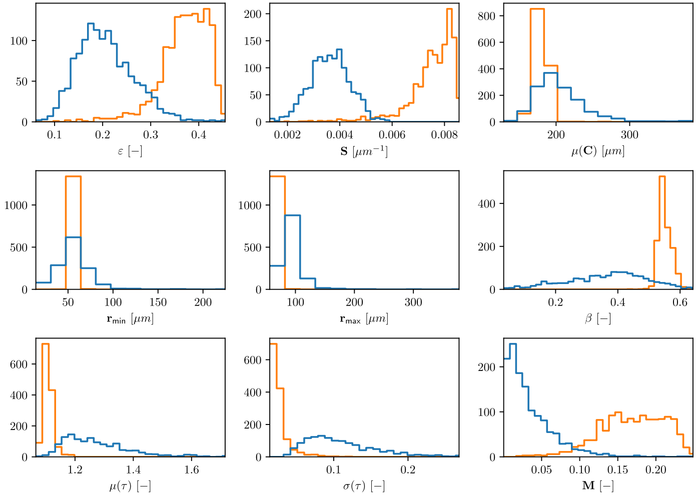

Histograms of various geometric descriptors and *M*-factors computed on small cutouts from CT data of loam (blue) and sand (orange).

Statistical description of data

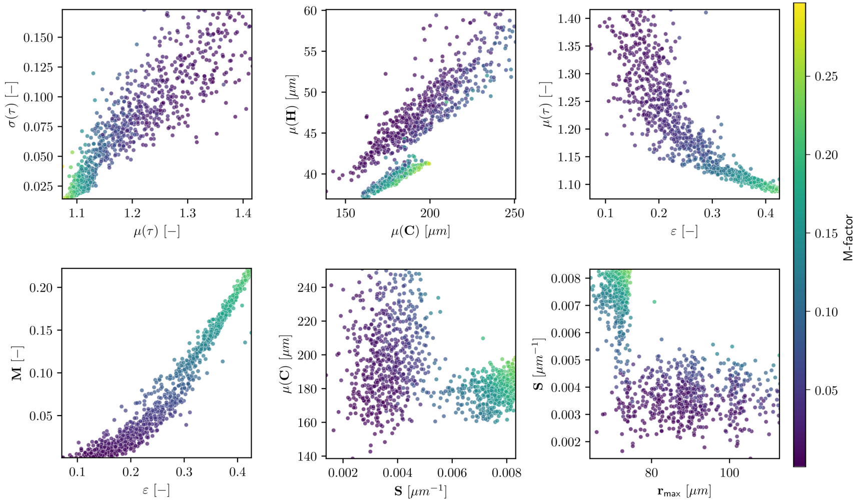

M-factor (color) as a function of pairs of geometric descriptors.

Functional relationships

Various candidates for prediction formulas for the M-factor are fitted to the data:

$$\widehat{M}_1 = \varepsilon^{c_1}, \quad \widehat{M}_2 = c_1 \varepsilon^{c_2}, \quad \widehat{M_3} = c_1 e^{c_2 \varepsilon}, \quad \widehat{M}_4 = \varepsilon^{c_1} \beta^{c_2} \mu(\tau)^{c_3},$$
$$\widehat{M}_5 = \varepsilon^{c_1 + c_2 \beta} \mu(\tau)^{c_3}, \quad \widehat{M}_6 = c_1 \mu(\tau)^{c_2} \sigma(\tau)^{c_3} \varepsilon^{c_4}, \quad \widehat{M}_7 = \varepsilon^{c_1} S^{c_2} r_{\max}^{c_3}$$

For evaluation, the R^2 and mean average percentage error are computed for each formula.

Functional relationships: Evaluation

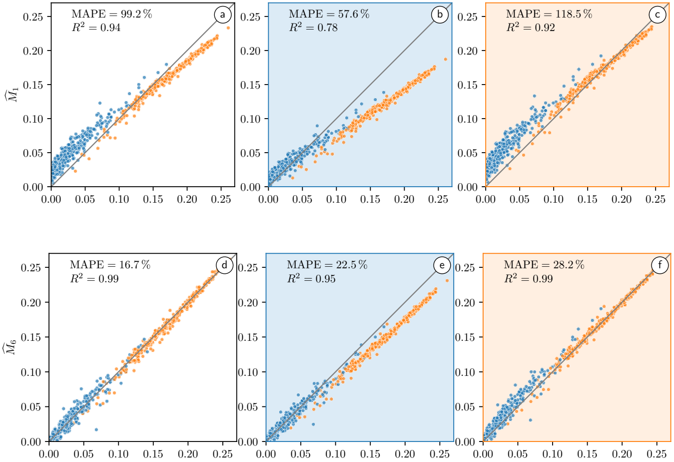

M-factor versus predicted M-factor $\hat{M}_i$. The colors of data points represent loam (blue) and sand (orange), respectively. The parameter values of regression formulas have been fitted on the entire training data (left), loam (center) and sand (right).

Functional relationships: Evaluation

$$\widehat{M}_1 = \varepsilon^{c_1}$$

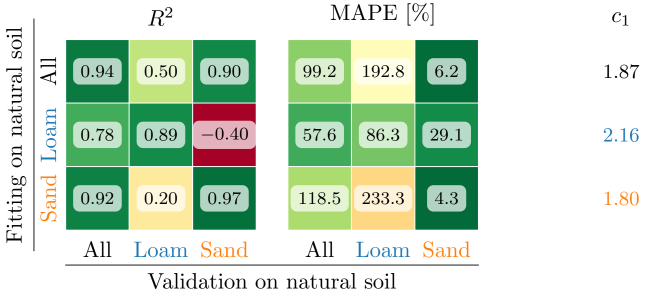

Fitting on natural soil	R^2 All	R^2 Loam	R^2 Sand	MAPE [%] All	MAPE [%] Loam	MAPE [%] Sand	c_1
All	0.94	0.50	0.90	99.2	192.8	6.2	1.87
Loam	0.78	0.89	−0.40	57.6	86.3	29.1	2.16
Sand	0.92	0.20	0.97	118.5	233.3	4.3	1.80

Validation on natural soil

Functional relationships: Evaluation

$$\widehat{M}_6 = c_1 \mu(\tau)^{c_2} \sigma(\tau)^{c_3} \varepsilon^{c_4}$$

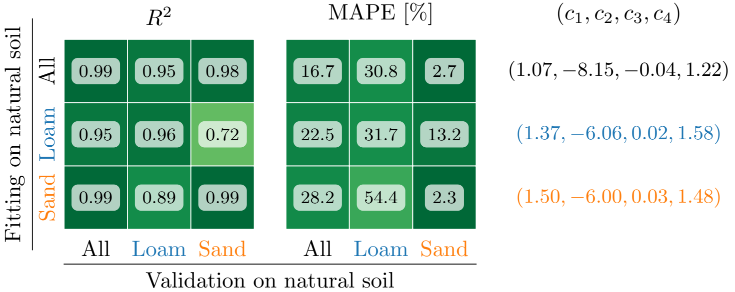

Fitting on natural soil	R^2 All	R^2 Loam	R^2 Sand	MAPE [%] All	MAPE [%] Loam	MAPE [%] Sand	(c_1, c_2, c_3, c_4)
All	0.99	0.95	0.98	16.7	30.8	2.7	$(1.07, -8.15, -0.04, 1.22)$
Loam	0.95	0.96	0.72	22.5	31.7	13.2	$(1.37, -6.06, 0.02, 1.58)$
Sand	0.99	0.89	0.99	28.2	54.4	2.3	$(1.50, -6.00, 0.03, 1.48)$

Validation on natural soil

Conclusion

Summary

- Level sets of Gaussian random fields were used to model the 3D microstructure of soil.
- By considering a wide variety of soil samples, formulas were be obtained which predict diffusion based on geometric descriptors.

Outlook

- As only a limited amount of measured data is available, the model can be used to simulate virtual, yet realistic soil structures with an even wider range of properties.
- Using this data, the prediction formulas can be validated and improved for not yet seen soil types.

Literature

- B. Prifling, M. Weber, N. Ray, A. Prechtel, M. Phalempin, S. Schlüter, D. Vetterlein, V. Schmidt, Quantifying the impact of 3D pore space morphology on soil gas diffusion in loam and sand. *Transport in Porous Media*, vol. 149, 501–527, 2023.
- M. Weber, B. Prifling, N. Ray, A. Prechtel, M. Phalempin, S. Schlüter, D. Vetterlein, V. Schmidt, Investigating relationships between 3D pore space morphology and soil gas diffusion based on data-driven spatial stochastic modeling. *Working paper* (under preparation).
- N. Ray, A. Rupp, R. Schulz, and P. Knabner, Old and new approaches predicting the diffusion in porous media. *Transport in Porous Media*, vol. 124, 803–824, 2018.
- M. Phalempin, E. Lippold, D. Vetterlein, and S. Schlüter, Soil texture and structure heterogeneity predominantly governs bulk density gradients around roots. *Vadose Zone Journal*, vol. 20, no. 5, e20147, 2021.